Materials Research Express

PAPER

# Structural, morphological and 6 MeV energy electron dosimetric properties of Cu doped $SnO_2$ phosphor



Materials Research Express

PAPER

# Structural, morphological and 6 MeV energy electron dosimetric properties of Cu doped $SnO_2$ phosphor

**Mahesh S Bhadane**[1], **Kishor H Gavhane**[1], **Ashish B Thorat**[1], **Ramakant P Joshi**[2], **Kaushik T Katre**[3], **Shailendra S Dahiwale**[1,4], **Vasant N Bhoraskar**[1] and **Sanjay D Dhole**[1,4]

[1] Microtron Accelerator Laboratory, Department of Physics, Savitribai Phule Pune University, Pune-411007, India
[2] Department of Physics, Annasaheb Magar Mahavidyalaya, Hadapsar, Pune-411028, India
[3] IUAC, Aruna Asaf Ali Marg, New Delhi-110067, India
[4] Authors to whom any correspondence should be addressed.

**E-mail:** ssd@physics.unipune.ac.in **and** sanjay@physics.unipune.ac.in

**RECEIVED**
26 November 2018

**REVISED**
16 January 2019

**ACCEPTED FOR PUBLICATION**
17 January 2019

**PUBLISHED**
1 February 2019

**Keywords:** $SnO_2$, hydrothermal method, electron irradiation, thermoluminescence, Microtron Accelerator

Supplementary material for this article is available online

## Abstract

Cu doped $SnO_2$ ($SnO_2$:Cu) nano phosphor (NP) was successfully synthesized by one-step simple hydrothermal method and it was characterized by XRD (x-ray Diffraction) for structural, FESEM (Field Emission Scanning Electron Microscopy) for morphological and EDS (Electron Dispersive Spectroscopy) for elemental analysis. NP was annealed at 700 °C for 2 h and its crystallinity for tetragonal phase was confirmed through XRD. The crystallite size was ~10.39 nm for un-annealed and ~18.16 nm for annealed samples which has been calculated using Scherer equation. The particle size was estimated to be ~43 nm and the elemental composition of Sn, O, Cu was obtained by EDS. In addition, to study the dosimetric properties, the $SnO_2$:Cu phosphors were irradiated with 6 MeV electron beam at fluences ranging from $10 \times 10^{11}$ e $cm^{-2}$ to $20 \times 10^{12}$ e $cm^{-2}$ which is equivalent to the 1.55 kGy to 31 kGy. The irradiated sample showed Thermoluminescence (TL) dosimetric glow peaks at 170 °C, 263 °C and 303 °C. $SnO_2$:Cu NP was found to be sensitive enough for energetic electrons. Further, it has been noticed that the TL dose response found sensitive upto $10 \times 10^{12}$ e $cm^{-2}$ (15.50 kGy) with fading of 5.1% for 2 months. Hence, $SnO_2$:Cu can be used for the measurement of electron doses.

## 1. Introduction

Numerous applications have been provided by metal-oxide semiconductor because of their suitable band gap which varies between 2.6 to 4.2 eV [1, 2]. Among several metal-oxides, $SnO_2$ has unique physiochemical properties [3, 4]. It is a n-type semiconductor materials provides great importance in broad range of applications, viz. gas and UV sensing [5–7], anode of lithium-ion battery [8–10], waste water purification [11], solar cell, and photo catalyst [12–14] etc. On the other hand, in the field of luminescence, efforts are being made to develop phosphors to change their optical and electronic properties by reducing the dimension of materials particle [15, 16].

Different doping of $SnO_2$ (nanosized phosphor) shows numerous applications like orange-red-emission for white light LEDs [17], energy transfer mechanism [18], thermoluminescence dosimetric (TLD) areas [19–21] etc. Some of the cases pure $SnO_2$ (without doping) also shows excellent characteristics of luminescent devices [22]. To prepare $SnO_2$ compounds, there are various routs adopted for different morphologies which can be used for various applications [5, 8, 23–25]. To mentioned few, Bajpayi *et al* [26] and Bhadane *et al* [15] have studied TLD properties through $\gamma$-irradiation on $SnO_2$:Eu nanoparticles. Zeferino *et al* [21] proposed a dose enhancing properties using $\beta$-irradiation for the radiotherapy applications. Dosimetry (D) is tool to measured the absorbed ionizing radiation and Thermoluminescence (TL) is the system to emits the light during heating the previously irradiated material i.e. insulator or semiconductor, with uniform heating temperature [27–29].

Further, Jiao *et al* [30] has studied electron beam irradiation effect on $SnO_2$ particles for the gas sensor application which they synthesized by spray pyrolysis route. But, no study has been done so far in the dosimetric field using high energy electron beam for $SnO_2$ nanophosphors, even though it has suitable dosimetric properties. Therefore, the aim of the current study is to prepare and investigate the Cu doped $SnO_2$ NPs for the electron dosimetry applications. The TL dosimetric properties of $SnO_2$:Cu have been studied by 6 MeV electrons (Race Track Microtron Accelerator). This study reveals some important features about the dosimetric properties of $SnO_2$:Cu nanophosphors (NP's).

## 2. Experimental procedure

### 2.1. Synthesis of $SnO_2$:Cu NPs

Copper doped Tin Oxide NPs were prepared by simple hydrothermal method [19]. All precursor was purchased as AR grade solution and used it for system of $SnO_2$:Cu NPs. At first the precursor, 20 ml solution of tin chloride ($SnCl_4.5H_2O$) and 60 ml solution of ammonium hydroxide (NaOH) was prepared in double distilled water (DDW) under continuous stirring condition. Magnetic stirring was performed for 30 min for both the aqueous solution. The NaOH solution was taken into burette and added to the $SnCl_4.5H_2O$ solution drop by drop until the pH of the resulting solution reach to 7. Subsequently, we added a 1 mol% $CuCl_2$ precursor (as Cu dopant which act as an activator) into the above resulting solutions under continues stirring and then added 50 ml ethanol (absolute, 99.99) in the mixture of $SnCl_4$ and NaOH respectively. The homogeneous mixture solution was then transferred to Teflon lined stainless steel autoclave having the capacity of 100 ml, and put into the oven at 180 °C for 24 h. After the hydrothermal reaction was complete, white precipitate (ppt) was collected. The ppt was filter out, wash with DDW and ethanol to remove the unreacted compounds from the wet ppt. At the end, the wet ppt was dried at 140 °C for 5 h under ambient condition. The obtained dried powder was denoted as $SnO_2$:Cu. The final powder (i.e. $SnO_2$:Cu phosphor) was used for further characterizations and TL studies. Two sets of samples prepared for characterization in which one set of samples was annealed at 700 °C and another set was kept un- annealed.

### 2.2. Characterization

The structural analysis was obtained using the x-ray Diffraction spectrometer (Bruker-AXS D8 ADVANCE) and morphological nature with elemental analysis was studied by Field Emission Scanning Electron Microscope & Energy Dispersive x-ray Spectrometer (FESEM: FEI Nova Nano SEM 450 & EDS:Bruker X-Flash 6I30) operated at 15 kV. The dosimetric properties of 6 MeV electron irradiated $SnO_2$:Cu phosphor was recorded using Nucleonix TLD reader having a heating rate ($\beta$) = 5 °C $s^{-1}$. The schematic of electron radiation source (6 MeV race track microtron) is shown in supplementary data file (figure S1 is available online at stacks.iop.org/MRX/6/055901/mmedia) [31]. The phosphors were irradiated in the air by keeping them on a Faraday cup at a distance of 12 cm from the extraction port of the microtron and the fluence was recorded in terms of counts, where, 1 count is nearly equal to $10^{11}$ electron. The dose conversion of electron fluence ($e^-/cm^2$) to Gray (Gy) information was indicates in supplementary data file (table S1).

## 3. Results and discussion

### 3.1. XRD analysis

Figure 1 depicts the XRD spectra of the pristine and annealed Cu-doped $SnO_2$ nanoparticles. The typical XRD pattern of the $SnO_2$:Cu NPs annealed at 700 °C exhibit all standards hkl peaks i.e. 26.55, 33.90, 37.85, 42.70, 51.75, 57.85, 57.85, 61.85, 64.80, 65.90, 71.35, 78.75, and 83.8 respectively corresponding to (110), (101), (200), (111), (210), (211), (220), (310), (002), (112), (301), (202) and (321). Data is in good agreement with the tetragonal phase and perfectly matches with the standard ICDD data (card no. 72-1147). The lattice constants $a$ = 0.4736 nm and $c$ = 0.3184 nm. The crystallite size calculated using Scherrer formula from (110) hkl peak was ~18.16 nm. From figure 1, it is observed that the crystallinity of tin oxide increases with annealing temperature. It happened, generally, after the annealing smaller particles get agglomerate with each other and make bigger one which increase crystallinity as well as peak intensity. This temperature has optimized after several experiments (not shown here). Moreover, no phase transformation observed after the annealing.

### 3.2. FESEM

Figure 2 shows the FESEM image of the Cu doped $SnO_2$ NPs. As seen from figure 2, the $SnO_2$:Cu NPs are spherical shape with a size range less than 43 nm which obtained using Image J software. The physical composition of Cu doped $SnO_2$ materials and its elemental distribution carried out through EDX elemental mapping and it is shown in supplementary data file (figure S2).

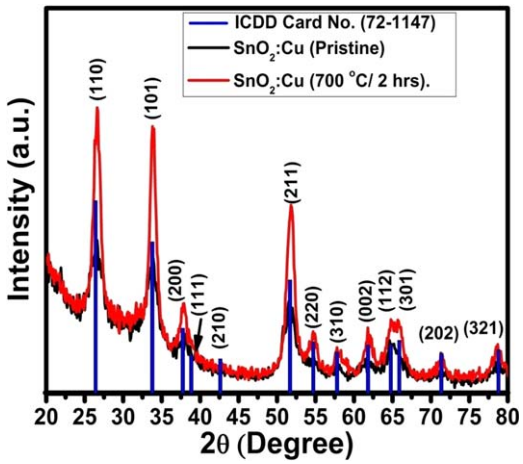


**Figure 1.** The XRD spectra of Cu doped $SnO_2$ NPs.

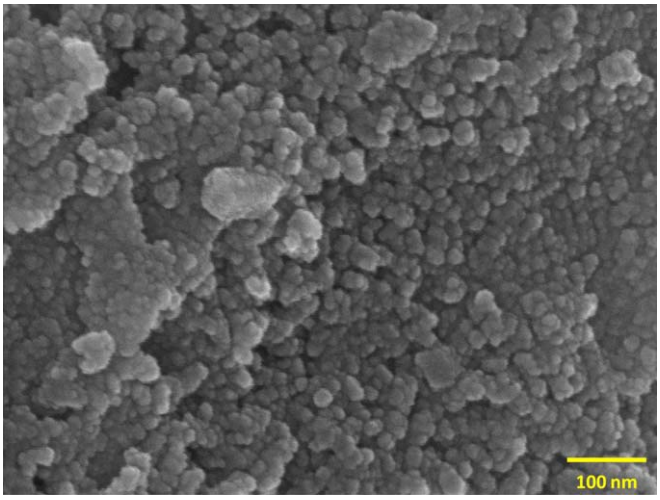


**Figure 2.** FESEM image of $SnO_2$:Cu NPs.

### 3.3. Thermoluminescence properties

*3.3.1. Glow curve and dose response*

The glow peak corresponds to the trap levels which are related to the impurity/defects. A shallow primary glow peak is observed at 93 °C. All others peaks ~170 °C and 270 °C can be associated to defects in the lattice and hence these peaks are dosimetric peaks which are well stable to store radiation. Here, we use electron beam to irradiate the cu doped $SnO_2$ NPs. Electron fluence was varied from $10 \times 10^{11}$ e $cm^{-2}$ to $20 \times 10^{12}$ e $cm^{-2}$ (i.e. 1.55 kGy to 31 kGy). Figure 3(a) showed glow curves irradiated with different doses i.e. (i) 1.55 kGy, (ii) 3.87 kGy, (iii) 11.62 kGy, (iv) 15.50 kGy, (v) 23.25 kGy and (vi) 31 kGy respectively. The dose-response of glow curve observed to be linearly increasing with increase in electron fluence upto $10 \times 10^{12}$ e $cm^{-2}$ (i.e. 15.50 kGy) and further gets saturated as can be seen from figure 3(a) and linearity of TL response of $SnO_2$:Cu is shown in figure 3(b). The linear dose-response was taken by calculating the area under the curve of TL glow curves respectively.

*3.3.2. Fading*

In between sample irradiation and reading time, the TL counts can be influenced by natural atmospheric conditions and daylight. For the confirmation of fading, we irradiated our sample at the dose of $75 \times 10^{11}$ e $cm^{-2}$ (i.e. 11.625 kGy) and then checked the TL signals immediately. Remaining samples were stored in the black paper under atmospheric conditions and their TL signals were recorded after a period of 6 h, 12 h, 1 day, 5 day, 10 day, 15 day, 20 day, 30 day, 45 day and 60 day respectively. Figure 4 shows 5.1% fading after the period of 60 days (i.e. two month) and it is well under the acceptable limit.

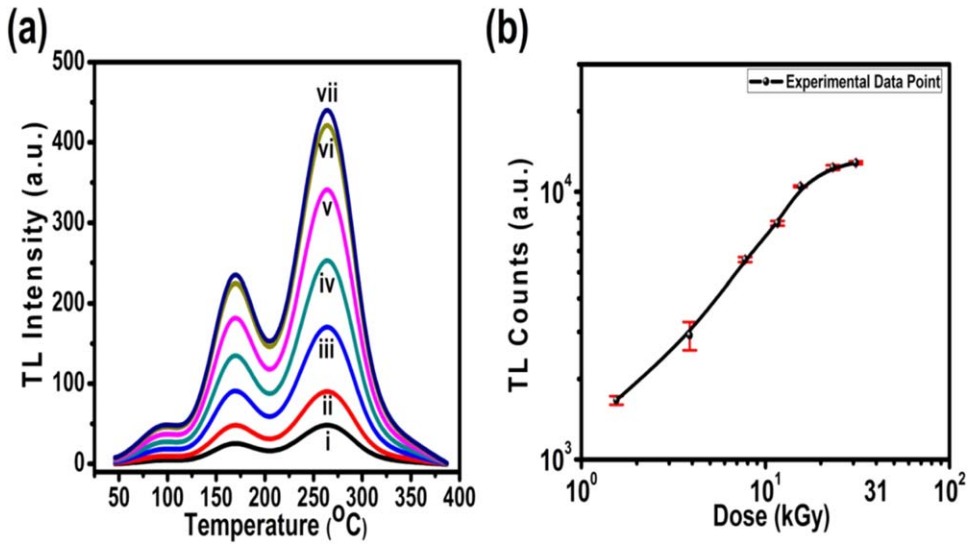


**Figure 3.** (a) Glow curve, and (b) linear dose response for 6 MeV electron irradiated $SnO_2$:Cu NPs.

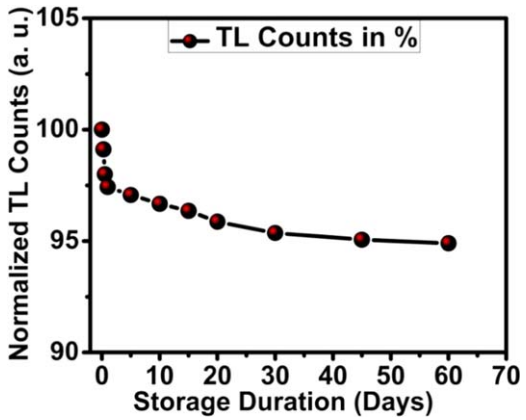


**Figure 4.** Thermoluminescence fading at the dose rate of 11.62 kGy for $SnO_2$:Cu NPs irradiated by 6 MeV electron beam.

*3.3.3. Reproducibility*

It is an important property to check the stability of dosimetric materials for the purpose of reuse. There are numerous phosphor materials which can be used many times with a minor fraction of changes to a repeated set of measurements like heating, irradiation, and counting the TL signals for constant dose exposure. Experimental results are shown in figure 5, where 6 samples of $SnO_2$: Cu NPs were exposed to a constant dose of $75 \times 10^{11}$ e $cm^{-2}$ (11.625 kGy) by electron source and observed stable results under the standard acceptable deviation (i.e. up to 5% range).

*3.3.4. GCD (glow curve deconvolution)*

The glow peaks of $SnO_2$:Cu irradiated samples are quite complicated and to analyze it the best way is peak fitting. Theoretical curves fitted with the experimental curve by using the glow curve deconvolution Spreadsheet software [32] using the famous Kitis equation [33].

G Kitis [33] have used very simple derivations of those functions and it confirms that the 1st order, 2nd order and general order of kinetics TL curve fitting. The good things in Kitis glow curve fitting functions is that most of the parameters are derived from the experimental glow curves and which become more reliable than the test values. The curve fitting was carried out using the first order, the second order and the general order equations as given below:

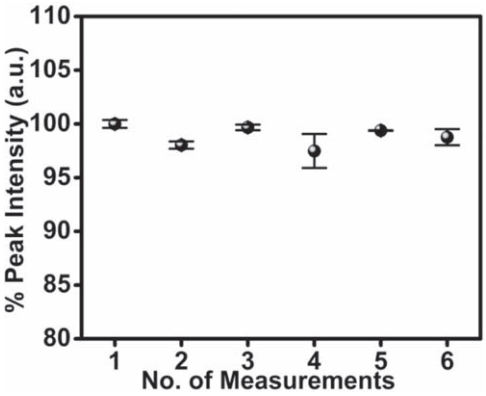


**Figure 5.** Reusability of $SnO_2$: Cu NPs of dose 11.625 kGy.

**For first order:**

$$I(T) = I_m \exp\left[1 + \frac{E}{kT}\frac{T - T_m}{T_m} - \frac{T^2}{T_m^2}\exp\left(\frac{E}{kT}\frac{T - T_m}{T_m}\right)\left(1 - \frac{2kT_m}{E}\right) - \frac{2kT_m}{E}\right] \quad (1)$$

**For second order:**

$$I(T) = 4I_m \exp\left(\frac{E}{kT}\frac{T - T_m}{T_m}\right)\left[\frac{T^2}{T_m^2}\exp\left(\frac{E}{kT}\frac{T - T_m}{T_m}\right)\left(1 - \frac{2kT}{E}\right) + 1 + \frac{2kT_m}{E}\right]^{-2} \quad (2)$$

**The general order:**

$$I(T) = I_m b^{\left(\frac{b}{b-1}\right)} \exp\left(\frac{E}{kT}\frac{T - T_m}{T_m}\right)\left[(b-1)\frac{T^2}{T_m^2}\left(1 - \frac{2kT}{E}\right)\exp\left(\frac{E}{kT}\frac{T - T_m}{T_m}\right) + 1 + (b-1)\frac{2kT_m}{E}\right]^{-\frac{b}{b-1}} \quad (3)$$

where, $I(T)$ = TL intensity at temperature T (K),

$I_m$ = maximum peak intensity,

$T_m$ = temperature corresponding to maximum peak intensity $I_m$,

E = trap depth or the thermal activation energy (eV) needed to free the trapped electrons,

B = order of kinetics, and

k = Boltzmann's constant ($8.6 \times 10^{-5}$ eVK$^{-1}$).

Moreover, the frequency factor (S) i.e. the lattice phonon vibrational frequency was also evaluated by the following general order equation:

The general order:

$$S = \frac{\beta E}{kT_m^2\left(1 + (b-1)\frac{2kT_m}{E}\right)}\exp\left(\frac{E}{kT_m}\right) \quad (4)$$

where, $\beta$ = linear heating rate (K/sec) and

b = Order of kinetics.

Figure of Merit (i.e. FOM) is another time one should take care while curve fitting, which is suggested by *Eddy* [34]. The *FOM* is the error function or a simple 'chi-square'. The 'best fit' is taken at which the error function converges to a minimum [35].

$$FOM = \sum_{J_f}^{J_i}\frac{|Y_j - Y(X_j)|}{A} \times 100 \quad (5)$$

where $J_i$ = initial temperature in the fit region,

$J_f$ = final or ending temperature in the fit region,

$Y_j$ = PMT tubes current at temperature j,

$Y(X_j)$ = Value of the function at channel j and

A = area under the peak, i.e., integral of the fit function between $J_i$ and $J_f$.

Here, Cu doped $SnO_2$ NPs samples irradiated to 15.5 kGy of 6 MeV electrons and deconvoluted it by Kitis equation. From figure 6, we found the four glow peaks, indicating four trapping levels. GCD fitting parameters

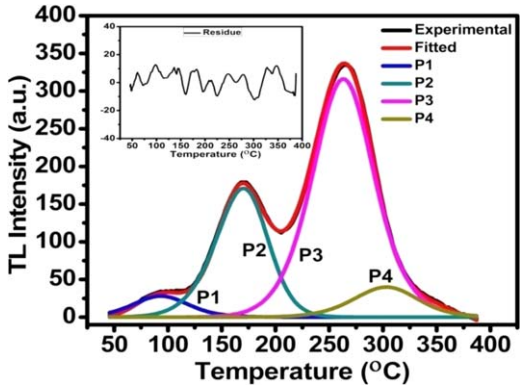


**Figure 6.** A typical analyzed glow curve of $SnO_2$:Cu measured after irradiation of 1000 counts (i.e. 15.5 kGy) by electron source.

**Table 1.** Data of $SnO_2$:Cu doped NPs on different trap depth parameters.

| Sample name | Peak | Peak temp. $T_m$ (°C) | Order of kinetics (b) | Trap depth E(eV) | Frequency factor $(s)^{-1}$ | FOM (%) |
|---|---|---|---|---|---|---|
| $SnO_2$:Cu (15.5 kGy) | **P1** | 93 | 1.60 | 0.54 | $4.54 \times 10^7$ | 1.67 |
| | **P2** | 170 | 1.36 | 0.79 | $1.97 \times 10^9$ | |
| | **P3** | 263 | 1.70 | 1.1 | $4.91 \times 10^{10}$ | |
| | **P4** | 303 | 1.58 | 1.18 | $4.36 \times 10^{10}$ | |

such as the trap depth (eV), Order of kinetics (b) and FOM as evaluated are shown in the consolidated form in table 1.

## 4. Conclusions

Cu doped $SnO_2$ phosphor has been successfully synthesized by hydrothermal technique. XRD results confirm the tetragonal phase and crystallite size around ~38 nm. FESEM–EDS revealed the particle size (i.e. $<$ 43 nm) and elemental mapping confirms the Stoichiometric ratio. TL dosimetric properties of $SnO_2$:Cu were studied using electron beam of 6 MeV Race-Track Microtron Accelerator. TL peak intensity increases with increase in electron beam dose from 1.55 kGy to 15.50 kGy after which it gets saturated. Moreover, the reproducibility shows good stability and fading is within the acceptable limit. Other useful dosimetric parameters also extracted from the glow curve deconvolution (GCD) method. These results reveal the possibility of using Cu doped $SnO_2$ phosphor in electron beam TL dosimetry.

## Acknowledgments

MSB is grateful to UGC, New Delhi, Government of India for granting UGC-BSR fellowship and financial assistance to carry out this work. SSD is acknowledged to BCUD, SPPU, Pune, for financial support to carry out this work.

## ORCID iDs

Sanjay D Dhole https://orcid.org/0000-0003-1696-5926

## References

[1] Zhengh W, Ding R, Yan X and He G 2017 Induced tunable morphology and band gap of ZnO *Mater. Lett.* **201** 85–8
[2] Yang C, Lee S, Chen S and Lin T 2006 The effect of annealing treatment on microstructure and properties of indium tin oxides films *Mater. Sci. Enginee.:* B **129** 154–60
[3] Guo J, Liu X, Wang H, Sun W and Sun J 2017 Synthesis of hollow tubular reduced graphene oxide/$SnO_2$ composites and their gas sensing properties *Mater. Lett.* **209** 102–5
[4] Batzill M and Diebold U 2005 The surface and materials science of tin oxide *Progr. Surf. Sci.* **79** 47–154
[5] Gupta P and Sharma S K 2017 A study of oxygen gas sensing in Zn-doped $SnO_2$ nanostructures *Mater. Res. Express* **4** 065010

[6] Aleksander G 2011 Nanosensors: towards morphological control of gas sensing activity. $SnO_2$, $In_2O_3$, ZnO and $WO_3$ case studies *Nanoscale* **3** 154
[7] Paulowicz I *et al* 2015 Three-dimensional $SnO_2$ nanowire networks for multifunctional applications: from high-temperature stretchable ceramics to ultraresponsive sensors *Adv. Electron. Mater.* **1** 1500081
[8] Faramarzi M S, Abnavi A, Ghasemi S and Sanaee Z 2018 Nanoribbons of $SnO_2$ as a high performance Li-ion battery anode material *Mater. Res. Express* **5** 065040
[9] Wang C, Zhou Y, Ge M Y, Xu X B, Zhang Z L and Jiang J Z 2012 Large-scale synthesis of $SnO_2$ nanosheets with high lithium storage capacity *J. Am. Chem. Soc.* **132** 46
[10] Lee K T, Lytle J C, Ergang N S, Oh S M and Stein A 2005 Synthesis and rate performance of monolithic macroporous carbon electrodes for lithium-ion secondary batteries *Adv. Funct. Mater.* **15** 547
[11] Zhao D and Wu X 2018 Nanoparticles assembled $SnO_2$ nanosheet photocatalysts for wastewater purification *Mater. Lett.* **210** 354–7
[12] Wang C, Zhao J C, Wang X M, Mai B X, Sheng G Y, Peng P A and Fu J M 2002 Preparation, characterization and photocatalytic activity of nano-sized ZnO/$SnO_2$ coupled photocatalysts *Appl. Catal. B: Environ.* **39** 269
[13] Vinodgopal K, Bedja I and Kamat P V 1996 Nanostructured semiconductor films for photocatalysis. Photoelectrochemical behavior of $SnO_2$/$TiO_2$ composite systems and its role in photocatalytic degradation of a textile azo dye *Chem. Mater.* **8** 2180
[14] Wang G, Lu W, Li J H, Choi J, Jeong Y, Choi S Y, Park J B, Ryu M K and Lee K 2006 V-shaped tin oxide nanostructures featuring a broad photocurrent signal: an effective visible-light-driven photocatalyst *Small* **2** 1436
[15] Zulfiqar, Yuan Y, Jiang Q, Yang J, Feng L, Wang W, Ye Z and Lu J 2016 Erratum to: variation in luminescence and bandgap of Zn-doped $SnO_2$ nanoparticles with thermal decomposition *J. Mater Sci: Mater Electron* **28** 13248–9
[16] Mehar B, Vishakha K, Akshey K, Mandeep S and Raj M B 2016 Structural and photoluminescence properties of tin oxide and tin oxide: C core–shell and alloy nanoparticles synthesized using gas phase technique *AIP Adv.* **6** 095321
[17] Zhai Y, Zhao Q, Han Y, Wang M and Yu J 2016 Hydrothermal synthesis, characterization and luminescence properties of orange—red-emitting phosphors $SnO_2$: Eu *Journal of Mater. Sci.: Mater. Electro.* **27** 677–84
[18] Del-Castillo J, Rodríguez V D and Mendez-Ramos J 2007 Energy transfer from the host to $Er^{3+}$ dopants in semiconductor $SnO_2$ nanocrystals segregated in sol–gel silica glasses *J. Nanopar. Res.* **10** 499–506
[19] Bhadane M S *et al* 2017 Synthesis and TSL properties of $SnO_2$:Eu nanophosphor for high gamma dosimetry *J. Alloys Comp.* **695** 1918–23
[20] Kumar V and Nagarajan R 2012 Thermoluminescence in heavily F-doped of $SnO_2$ nanocrystals *Chem. Phys. Lett.* **530** 98–101
[21] Sánchez Zeferino R, Pal U, Melendrez R, Durán-Muñoz H A and Flores M B 2013 Dose enhancing behavior of hydrothermally grown Eu-doped $SnO_2$ nanoparticles *J. Appl. Phys.* **113** 64306
[22] Feng G, Wang S F, Meng K L, Guang J Z, Dong X and Duo R Y 2004 Photoluminescence properties of $SnO_2$ nanoparticles synthesized by sol-gel method *J. Phys. Chem.* B **108** 8119–23
[23] Chen J *et al* 2008 Structure and photoluminescence property of Eu-doped $SnO_2$ nanocrystalline powders fabricated by sol–gel calcination process *J. Phys. D: Appl. Phys.* **41** 105306
[24] Wang C, Zhou Y, Ge M, Xu Z and Jiang J Z 2010 Large-scale synthesis of $SnO_2$ nanosheets with high lithium storage *J. Amer. Chemi. Soc.* **132** 46–7
[25] Maestre D, Cremades A and Piqueras J 2005 Growth and luminescence properties of micro- and nanotubes in sintered tin oxide *J. Appl. Phys.* **97** 44316
[26] Bajpai N, Khan S A, Kher R S, Bramhe N, Dhoble S J and Tiwari A 2014 Thermoluminescence investigation of sol–gel derived and $\gamma$ -irradiated $SnO_2$: $Eu^{3+}$ nanoparticles *J. Lumin.* **145** 940–3
[27] Bhatt B C and Kulkarni M S 2013 Worldwide status of personnel monitoring using thermoluminescent (TL), optically stimulated luminescent (OSL) and Radiophotoluminescent (RPL) dosimeters *Int J. Lumin. Appli.* **3** 6
[28] Mckeever S W S 1988 *Thermoluminescence of Solids* (Cambridge, UK: Cambridge University Press) pp 392
[29] Chen R and McKeever S W S 1997 *Theory of Thermoluminescence and Related Phenomena.* (Singapore: World Scientific) pp 576
[30] Jiao Z, Wan X, Zhao B, Guo H, Liu T and Wu M 2008 Effects of electron beam irradiation on tin dioxide gas sensors *Bull. Mater. Sci.* **31** 83–6
[31] Sunitha D V, Nagabhushana H, Hareesh K, Bhoraskar V N and Dhole S D 2017 Tailoring the luminescence properties of $Y_2O_3$:$Sm^{3+}$ nanophosphors by 6 MeV electron beam irradiation *Rad. Measur.* **96** 19–28
[32] Afouxenidis D, Polymeris G S, Tsirliganis N C and Kitis G 2012 Computerised curve deconvolution of TL/OSL curves using a popular spreadsheet program *Radiat. Prot. Dosim.* **149** 363–70
[33] Kitis G, Gomez-Ros J M and Tuyn J W N 1998 Thermoluminescence glow-curve deconvolution functions for first, second and general orders of kinetics *J. Phys. D: Appl. Phys.* **31** 2636
[34] Balian H G and Eddy N W 1977 figure-of-merit (FOM), an improved criterion over the normalized chi-squared test for assessing goodness-of-fit of gamma-ray spectral peaks *Nucl. Instr. Meth.* **145** 389–95
[35] Sunta C M 2015 *Unraveling Thermoluminescence* (*Springer Series in Material Science*) vol 202 (Berlin: Springer) pp 1–188